Proc. Natl. Acad. Sci. USA
Vol. 92, pp. 11686–11690, December 1995
Biochemistry

The LAR/PTPδ/PTPσ subfamily of transmembrane protein-tyrosine-phosphatases: Multiple human LAR, PTPδ, and PTPσ isoforms are expressed in a tissue-specific manner and associate with the LAR-interacting protein LIP.1

(alternative splicing/immunoglobulin superfamily/protein tyrosine phosphorylation)

RAFAEL PULIDO*, CARLES SERRA-PAGÈS†, MAY TANG‡, AND MICHEL STREULI*

‡Division of Tumor Immunology, Dana–Farber Cancer Institute, 44 Binney Street, Boston, MA 02115; and Departments of *Pathology and †Medicine, Harvard Medical School, Boston, MA 02115

Communicated by Stuart F. Schlossman, Dana–Farber Cancer Institute, Boston, MA, September 7, 1995

ABSTRACT **The transmembrane protein-tyrosine-phosphatases (PTPases) LAR, PTPδ, and PTPσ each contain two intracellular PTPase domains and an extracellular region consisting of Ig-like and fibronectin type III-like domains. We describe the cloning and characterization of human PTPσ (HPTPσ) and compare the structure, alternative splicing, tissue distribution, and PTPase activity of LAR, HPTPδ, and HPTPσ, as well their ability to associate with the intracellular coiled-coil LAR-interacting protein LIP.1. Overall, these three PTPases are structurally very similar, sharing 64% amino acid identity. Multiple isoforms of LAR, HPTPδ, and HPTPσ appear to be generated by tissue-specific alternative splicing of up to four mini-exon segments that encode peptides of 4–16 aa located in both the extracellular and intracellular regions. Alternative usage of these peptides varies depending on the tissue mRNA analyzed. Short isoforms of both HPTPσ and HPTPδ were also detected that contain only four of the eight fibronectin type III-like domains. Northern blot analysis indicates that LAR and HPTPσ are broadly distributed whereas HPTPδ expression is largely restricted to brain, as is the short HPTPσ isoform containing only four fibronectin type III-like domains. LAR, HPTPδ, and HPTPσ exhibit similar *in vitro* PTPase activities and all three interact with LIP.1, which has been postulated to recruit LAR to focal adhesions. Thus, these closely related PTPases may perform similar functions in various tissues.**

Protein-tyrosine-phosphatases (PTPases) are a structurally diverse family of transmembrane and intracellular-type enzymes that together with protein-tyrosine kinases regulate protein tyrosine phosphorylation (1). Tyrosine phosphorylation of signaling molecules, such as enzyme and adapter proteins or cytoskeleton-associated proteins, is intimately associated with diverse cellular processes, including activation, proliferation, differentiation, and migration (2–4). Transmembrane-type PTPases contain extracellular regions of varying architecture connected to one or two intracellular PTPase domains via a transmembrane peptide (5). This structure suggests that these proteins play an important role in communicating information between the outside and inside of the cell. For instance, deficiencies in the expression of the CD45 transmembrane PTPase abrogate lymphocyte maturation and activation (6). Several closely related transmembrane PTPases, including LAR, PTPδ, PTPσ, PTPμ, and PTPκ, have extracellular regions comprising tandemly arranged Ig-like domains and fibronectin type III (FN III)-like domains (7–15). This extracellular-region architecture is also found in known cell adhesion molecules, including the neural cell adhesion molecule N-CAM (16) and in receptors for growth-regulatory proteins (17), suggesting that some of these transmembrane PTPases have similar ligands and thus function in regulating cell–cell or cell–matrix interactions. Consistent with such a role is the demonstration that PTPμ and PTPκ have homophilic binding properties (18–20). Further, LAR and the intracellular LAR-interacting protein LIP.1 colocalize at focal adhesions (21). We report the cloning and molecular characterization of the human PTPσ (HPTPσ) transmembrane PTPase§ and compare the tissue distribution and tissue-specific alternative splicing of HPTPσ with that of HPTPδ and LAR. Whereas HPTPσ, HPTPδ, and LAR are structurally very similar, there exist distinct patterns of tissue distribution and structural diversity within this subfamily of transmembrane-type PTPases. Further, HPTPσ and HPTPδ, like LAR, can interact with LIP.1, suggesting that these PTPases may serve similar functions in regulating cell–matrix interactions.

MATERIALS AND METHODS

cDNA Cloning and Sequencing. HPTPσ cDNA clones 55, 47, 16, and 31 (Fig. 1) were isolated from a λgt11 human fetal brain cDNA library (Clontech) essentially as described (15). HPTPσ cDNA clones 46.8, 62.1, and 75.1 (Fig. 1) were obtained by reverse transcription (RT)–PCR amplification (10) using RNA derived from human fetal lung FHs 738Lu cells (ATCC HTB 157) and human fetal brain (Clontech). HPTPσ cDNAs were subcloned into plasmid vectors prior to DNA sequence determination by the chain-termination method. The putative initiation methionine residue shown in Fig. 2*A* is encoded by nt 109–111.

Northern Blot Analysis. A tissue Northern blot containing about 2 μg of poly(A)$^+$ RNA per lane was obtained from Clontech and hybridized to ^{32}P-labeled DNA probes under conditions recommended by the supplier. The specificity of HPTPσ, HPTPδ, and LAR probes was confirmed by dot blot experiments using plasmid DNAs containing the various PTPase sequences (data not shown).

Detection of mRNA by RT–PCR. Poly(A)$^+$ RNA isolated from human kidney and fetal brain tissue was obtained from Clontech. Total RNA from FHs 738Lu and human umbilical vein endothelial cells (Clonetics, San Diego) was prepared by the guanidinium isothiocyanate method (22). RT–PCR (10) products were analyzed in 1.5% or 1.8% agarose gels. The

The publication costs of this article were defrayed in part by page charge payment. This article must therefore be hereby marked "*advertisement*" in accordance with 18 U.S.C. §1734 solely to indicate this fact.

Abbreviations: PTPase, protein-tyrosine-phosphatase; HPTPδ and HPTPσ, human PTPases δ and σ; FN-III, fibronectin type III; F4–F7, FN III-like domains 4–7; meA-meD, mini-exons A–D; RT, reverse transcription; GST, glutathione *S*-transferase.

§The HPTPσ sequence reported in this paper has been deposited in the GenBank database (accession no. U35234).

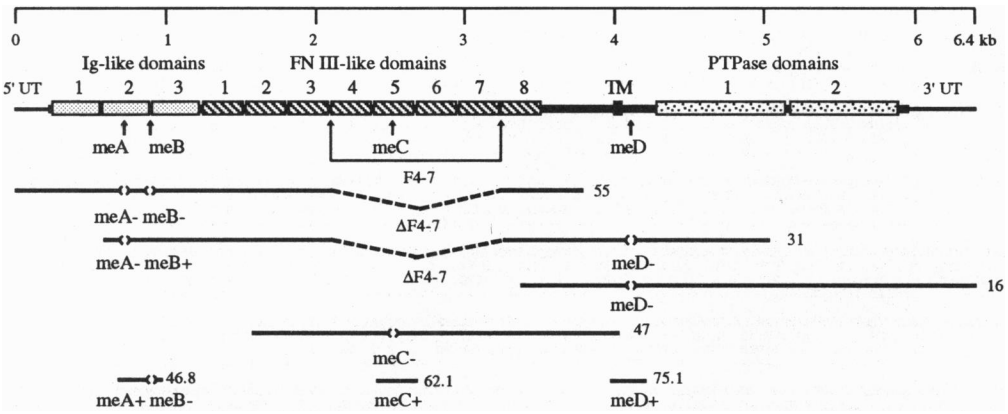

FIG. 1. Schematic structure of HPTPσ cDNA. At the top is a composite of 6.4-kb cDNA encoding HPTPσ which includes the relative positions of the 5′ untranslated (5′UT) and 3′ untranslated (3′UT) regions. The open reading frame encodes three Ig-like domains, eight FN III-like domains, the transmembrane peptide (TM), and two PTPase domains. Below the schematic, thick lines represent lengths and relative positions of the various HPTPσ cDNAs isolated. Dashed lines and brackets represent deleted sequences as compared with other cDNAs. The locations of the alternatively used mini-exon A–D (meA–meD) and FN III-like domain 4–7 (F4–F7) sequences are indicated with vertical arrows. Clones 46.8, 62.1, and 75.1 were derived by RT–PCR.

sequences of the synthetic oligonucleotide PCR primers are available upon request.

Preparation of PTPase Fusion Proteins and Phosphatase Assay. DNA sequences encoding cytoplasmic regions of LAR (7), HPTPδ (10), HPTPσ (Fig. 2*A*), and CD45 (23) were inserted into the polylinker region of pGEX.2T (Pharmacia) to create glutathione *S*-transferase (GST) fusion proteins (see Table 1). GST-PTPase fusion proteins were expressed in *Escherichia coli* NM522 and purified from bacterial lysates by use of glutathione-Sepharose beads (Pharmacia). Phosphatase activities of partially purified GST-PTPase fusion proteins were measured (24) using [^{32}P]phosphotyrosine-containing myelin basic protein (MBP) or Raytide peptide substrates. Substrates were labeled with [γ-^{32}P]ATP by the p56^{lck} tyrosine kinase (Upstate Biotechnology, Lake Placid, NY). The protein concentration of the various GST fusion proteins was determined by Coomassie staining.

Interaction Trap Assay. Plasmid DNAs and yeast strains used for the interaction trap assay were provided by Roger Brent and colleagues (Massachusetts General Hospital, Boston) and used as described (25). The regions of the LAR (7), HPTPδ (10), HPTPσ (Fig. 2*A*), CD45 (23), and LIP.1 (21) peptides fused to the LexA DNA-binding domain or B42 transcription-activation domain are given in Table 2.

Cell Transfections and Protein Analysis. COS-7 transfections were done with the expression vector pMT.2.LIP.1b, encoding LIP.1, or the control expression plasmid pMT.2 as described (21). Transfected COS-7 cells were metabolically labeled with [^{35}S]methionine and then lysed in 1% (vol/vol) Nonidet P-40/150 mM NaCl/50 mM Tris·HCl, pH 8.0/5 mM EDTA as described (21). Cell lysates were precleared with glutathione-Sepharose beads (Pharmacia), and samples (0.2 ml) of the lysates were incubated for 16 hr at 4°C with 1 μg of the GST fusion proteins (described above) before addition of glutathione-Sepharose beads for 2 hr at 4°C. The beads were washed with phosphate-buffered saline containing 0.1% Triton X-100, and the samples were analyzed by SDS/10% PAGE under reducing conditions. Immunoprecipitations using the anti-LIP.1 monoclonal antibody α-LIP.1.77 were done as described (21).

RESULTS AND DISCUSSION

Structure of HPTPσ. To isolate human transmembrane PTPases similar to LAR and HPTPδ, a human fetal brain cDNA library was screened with a mixture of LAR and HPTPδ cytoplasmic-region cDNA probes (7, 10) under nonstringent hybridization conditions. A cDNA clone thus isolated (clone 16, Fig. 1) encoded a peptide that was related to LAR and HPTPδ, but was most similar to rodent PTPσ (11, 12, 26–29). This cDNA was termed HPTPσ cDNA. Additional overlapping HPTPσ cDNA clones were isolated by using appropriate HPTPσ cDNA probes (clones 47, 31, and 55) or by isolation of RT–PCR-derived cDNA clones (clones 46.8, 62.1, and 75.1; Fig. 1). The longest composite cDNA spans 6.4 kb and contains a 5844-bp open reading frame encoding a protein of 1948 aa. The deduced amino acid sequence of this HPTPσ isoform is shown in Fig. 2*A* aligned with the human HPTPδ and LAR transmembrane PTPase sequences. As the N-terminal 29 aa are likely to serve as a signal peptide (31), the 30th amino acid (glutamic acid) is predicted to be the N terminus of the mature 1919-aa HPTPδ protein and is designated +1 (Fig. 2*A*). A hydrophobic stretch of 25 aa, residues 1253–1277 (underlined in Fig. 2*A*), is likely to be the transmembrane peptide. Sequence comparisons suggest that the 1252-aa extracellular region of HPTPσ comprises three Ig-like domains and 8 FN III-like domains. Four putative N-linked glycosylation sites are present (# in Fig. 2*A*), three of which are conserved in HPTPσ, HPTPδ, and LAR. HPTPσ contains two or three overlapping putative furin-like endoprotease cleavage sites located between aa 1161 and 1171 (pro.site in Fig. 2*A*), suggesting that HPTPσ, like HPTPδ, LAR, and rat PTPσ, is expressed on the cell surface as two subunits derived by proteolytic cleavage of a proprotein (10, 11, 32). The 642-aa HPTPσ intracellular region contains two PTPase domains. The overall amino acid sequence identity is 73% for HPTPσ vs. HPTPδ, 68% for HPTPσ vs. LAR, 71% for HPTPδ vs. LAR, and 93% for HPTPσ vs. mouse PTPσ (MPTPσ). The intracellular regions of HPTPσ, HPTPδ, and LAR share 82% amino acid identity. Thus, the overall architecture and sequence of HPTPσ are very similar to those of LAR and HPTPδ, and PTPσ is evolutionarily well conserved.

Isolation of cDNAs Encoding Multiple Isoforms of HPTPσ, HPTPδ, and LAR. Several of the HPTPσ cDNA clones isolated either contained or lacked sequences encoding short peptide regions designated meA–meD or lacked sequences encoding F4–F7 (Fig. 1), suggesting the existence of multiple HPTPσ isoforms that are generated by alternative splicing. This suggestion is consistent with previous results demonstrating the existence of two or more isoforms for rodent PTPσ (12, 26–29), mouse and human PTPδ (9, 10), and human and rat LAR (30, 33). To determine the extent to which the meA–meD and F4–F7 sequences were alternatively used by HPTPσ, HPTPδ, and LAR, RT–PCR analysis using primers flanking the alternatively used sequences was followed by sequence

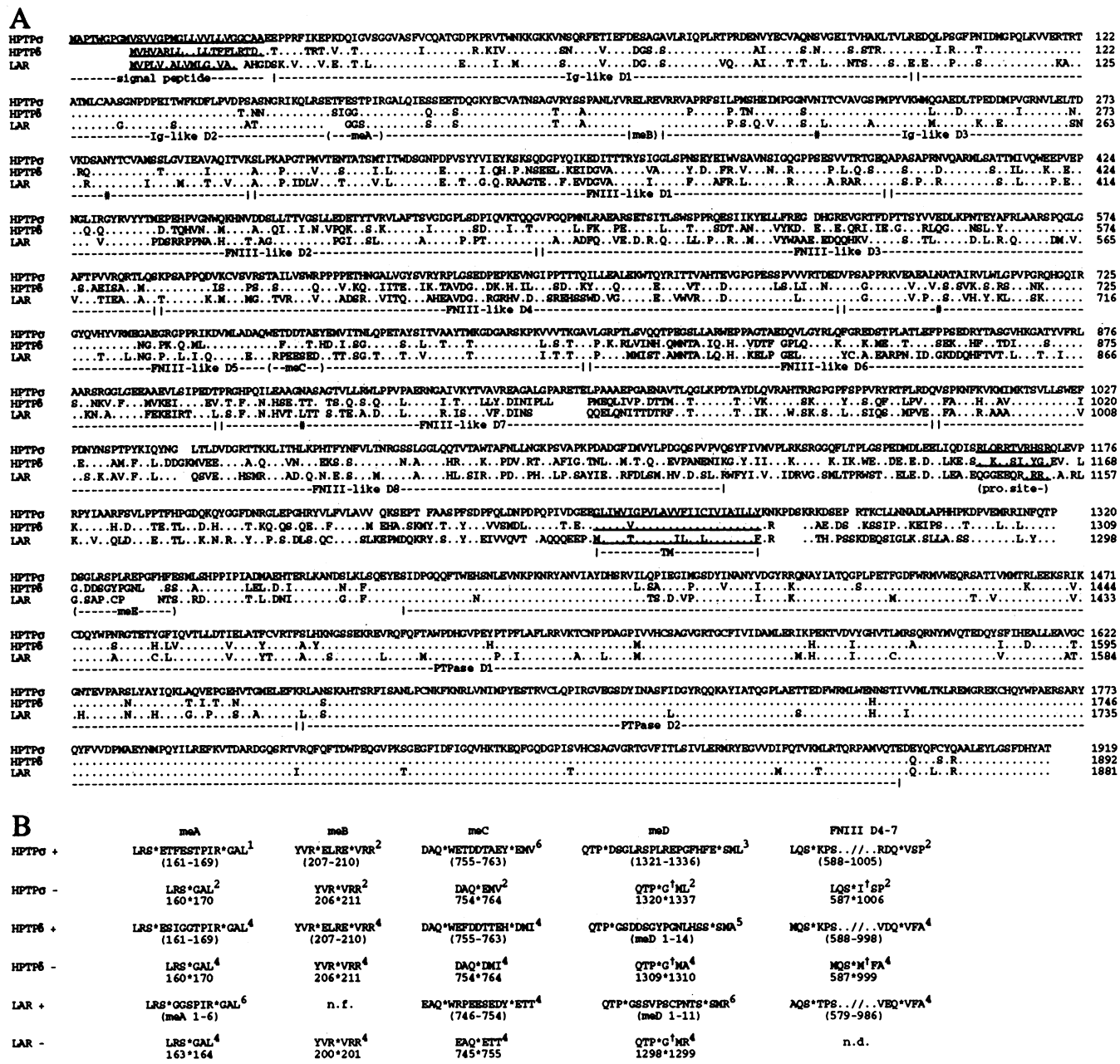

FIG. 2. Deduced primary structure of HPTPσ. (*A*) The HPTPσ amino acid sequence deduced from cDNA cloning is shown and is compared with the HPTPδ (10) and human LAR (7) sequences. The predicted signal peptide, transmembrane peptide (TM), and proprotein processing site (pro.site) are underlined. The extent and boundaries of the Ig-like domains, FN III-like domains, processing site, transmembrane peptide, and PTPase domains are indicated by dashes and vertical lines, respectively. The predicted domain junctions are based on the human *lar* gene organization (30). The relative positions of the alternatively used HPTPσ meA–meD peptides are shown, and putative N-linked glycosylation sites are indicated by #. Dots in the HPTPδ sequence and LAR sequence indicate identical amino acids with HPTPσ. Spaces in the sequences indicate gaps. (*B*) Deduced amino acid sequences of various HPTPσ, HPTPδ, and LAR cDNA clones isolated by RT–PCR analysis and/or cDNA cloning. Shown are amino acid sequences containing (+) or lacking (−) the sequences encoding the meA–meD peptides or F4–F7. The position of the sequence insertion or deletion is marked by stars. Numbering refers to the amino acid numbers shown in *A*. Superscripts designate the source of the amino acid sequence: 1, RT–PCR using FHs 738Lu RNA; 2, cDNA cloning using the fetal brain cDNA library and in most cases by RT–PCR using brain mRNA; 3, RT–PCR using brain and kidney mRNA; 4, cDNA cloning as described (7, 10, 30); 5, RT–PCR using human umbilical vein endothelial cell RNA; 6, RT–PCR using brain mRNA. n.f. indicates that these isoforms were not found by RT–PCR using brain, kidney, or human umbilical vein endothelial cell mRNA or by cDNA cloning. n.d., Not detected as determined by O'Grady *et al.* (30). † indicates that the change of amino acid between the sequence containing or lacking certain alternatively used sequences is probably the result of alternative splicing.

B	meA	meB	meC	meD	FNIII D4-7
HPTPσ +	LRS*ETFESTPIR*GAL[1] (161-169)	YVR*ELRE*VRR[2] (207-210)	DAQ*WETDDTAEY*EMV[6] (755-763)	QTP*DSGLRSPLREPGFHFE*SML[3] (1321-1336)	LQS*KPS..//..RDQ*VSP[2] (588-1005)
HPTPσ −	LRS*GAL[2] 160*170	YVR*VRR[2] 206*211	DAQ*EMV[2] 754*764	QTP*G†ML[2] 1320*1337	LQS*I†SP[2] 587*1006
HPTPδ +	LRS*ESIGGTPIR*GAL[4] (161-169)	YVR*ELRE*VRR[4] (207-210)	DAQ*WEFDDTTEH*DMI[4] (755-763)	QTP*GSDDSGYPGNLHSS*SMA[5] (meD 1-14)	MQS*KPS..//..VDQ*VFA[4] (588-998)
HPTPδ −	LRS*GAL[4] 160*170	YVR*VRR[4] 206*211	DAQ*DMI[4] 754*764	QTP*G†MA[4] 1309*1310	MQS*M†FA[4] 587*999
LAR +	LRS*GGSPIR*GAL[6] (meA 1-6)	n.f.	EAQ*WRPEESEDY*ETT[4] (746-754)	QTP*GSSVPSCPNTS*SMR[6] (meD 1-11)	AQS*TPS..//..VEQ*VFA[4] (579-986)
LAR −	LRS*GAL[4] 163*164	YVR*VRR[4] 200*201	EAQ*ETT[4] 745*755	QTP*G†MR[4] 1298*1299	n.d.

determination of the individual PCR products. In most cases, RT–PCR-derived cDNA or cDNA-library-derived cDNA was isolated that either contained or lacked the meA–meD sequences, as well as the F4–F7 sequences, for all three PTPases. The amino acid sequences determined for the alternatively used meA–meD and F4–F7 for HPTPσ, HPTPδ, and LAR are summarized in Fig. 2*B*. No LAR clones were isolated that contained the meB sequence. LAR isoforms lacking the F4–F7 sequences were also not detected (30), although a rat LAR isoform mRNA that lacks sequences encoding F4, F6, and F7 has been reported (33). All of these alternatively used sequences are inserted between exon–exon junctions based on the exon–intron organization of the human *lar* gene (30). The meA peptide is predicted to affect the length of a loop region

between the D and E β-strands of the second Ig-like domain, the meB peptide is predicted to affect the spacing between the second and third Ig-like domains (34), the meC peptide is located within the fifth FN III-like domain, and the meD peptide is located between the transmembrane peptide and the first PTPase domain (PTPase D1) (Fig. 2*A*). The alternative usage of F4–F7 presumably affects the distance between the Ig-like domains and the plasma membrane. The tissue-specific, alternative expression of the HPTPσ, HPTPδ, and LAR meD coding segment was analyzed by RT–PCR (Fig. 3). HPTPσ mRNA with or without the meD sequence (356 and 308 bp, respectively; confirmed by sequence analysis of PCR-generated cDNA) was present in both brain and kidney mRNA (lanes 3 and 4), whereas the predominant HPTPδ mRNA in both brain and kidney lacked the meD sequence (292 bp; lanes 6 and 7). LAR mRNA lacking the meD sequence predominated in the brain sample (312 bp; lane 9), whereas the kidney sample contained only the mRNA lacking the LAR meD sequence (279 bp; lane 10). Thus, the RT–PCR analysis and cDNA cloning demonstrate that all three members of the human LAR/PTPδ/PTPσ subfamily can generate a large number of isoforms by the tissue-specific inclusion or exclusion of the meA–meD peptides and F4–F7.

The functional significance of the existence of multiple HPTPσ, HPTPδ, and LAR isoforms is unclear, but presumably some isoforms (containing meA, meB, meC, and/or F4–F7) affect the interaction of these PTPases with their putative extracellular ligands, whereas others containing the meD peptide may affect interactions with intracellular proteins and/or PTPase activity. Some isoforms of N-CAM contain the 10-aa VASE peptide located within the fourth Ig-like domain. This alternatively used peptide regulates the neurite outgrowth-promoting activity of N-CAM (35). Small peptide insertions between the second and third Ig domains have been reported for other cell adhesion molecules, including the neural adhesion molecules Nr-CAM and neurofascin (36, 37). Thus, it seems likely that the meA–meC peptides regulate the interaction of the ectodomains of HPTPσ, HPTPδ, and LAR with their putative ligand(s). The intracellular meD peptide contains potential serine phosphorylation site(s), suggesting that phosphorylation of these site(s) might affect PTPase activity and/or interaction with substrates or other binding molecules.

Differential Tissue Distribution of HPTPσ, HPTPδ, and LAR mRNA. Northern blot analysis was performed with poly(A)$^+$ RNA isolated from various human tissues and gene-specific cDNA probes. HPTPσ mRNA (7.7 kb) was detected in all of the tissue samples tested except for placenta and liver (Fig. 4*A*). The brain sample also contained relatively high amounts of a 6.6-kb HPTPσ mRNA. A HPTPσ F4–F7-specific probe hybridized to the 7.7-kb mRNA but not to the 6.6-kb mRNA, suggesting that this shorter mRNA species encodes the HPTPσ isoform lacking F4–F7 (Fig. 4*B*). HPTPδ mRNA was predominantly detected in brain and, to a lesser extent, in heart, placenta, and kidney (Fig. 4*C*). These HPTPδ-positive tissues contained multiple HPTPδ mRNA species ranging in length from 7.9 to 11.2 kb. LAR mRNA expression was detected in all of the tissue samples tested except for skeletal muscle (Fig. 4*D*). In brain, LAR mRNA was 8.4 kb long, whereas in the other tissue samples it was 9.0 kb. The existence of different-length HPTPσ, HPTPδ, and LAR mRNAs is consistent with the generation of distinct PTPase isoforms by alternative splicing of pre-mRNA (see also Figs. 2 and 3). Taken together, these results indicate that the HPTPσ, HPTPδ, and LAR PTPases have overlapping but distinct tissue distribution and that PTPase isoforms are expressed in a tissue-specific manner.

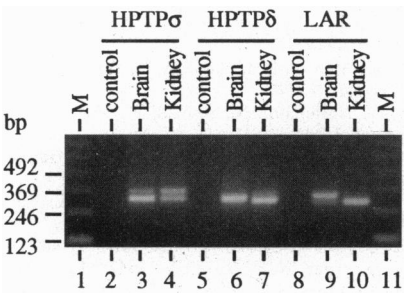

FIG. 3. Differential expression of HPTPσ, HPTPδ, and LAR mRNAs containing or lacking the meD sequence. RT–PCR analysis of poly(A)$^+$ RNA isolated from fetal brain and kidney tissues was performed with primers specific for HPTPσ, HPTPδ, or LAR. The various PCR products generated were subcloned into plasmid vectors and the nucleotide sequences were determined. Control indicates RT–PCR with no poly(A)$^+$ RNA template. Lane M, DNA size markers.

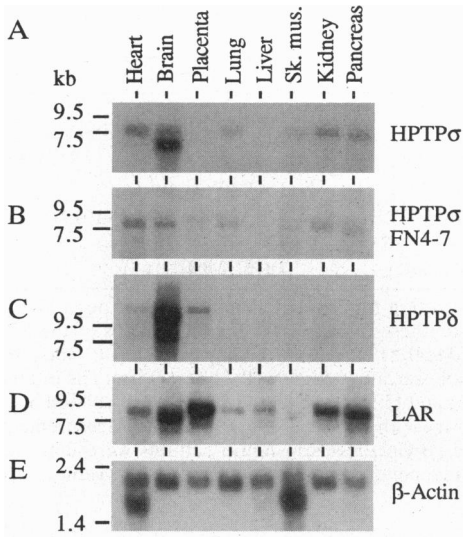

FIG. 4. Northern blot analysis of poly(A)$^+$ RNA from various human tissues with radiolabeled cDNA probes specific for HPTPσ (*A*), HPTPσ isoforms containing F4–F7 (*B*), HPTPδ (*C*), LAR (*D*), or β-actin (*E*). The HPTPσ cDNA probe spans nt 1777–1956 and 3215–3658, which encode aa 528–587 and 1006–1153 of the full-length HPTPσ isoform (Fig. 2*A*); the HPTPσ probe specific for F4–F7 spans nt 2158–2793, which encode aa 655–866; the HPTPδ cDNA probe spans nt 3157–3622, which encode aa 982–1136 (10); the LAR cDNA probe spans nt 1197–1921, which encode aa 260–501 (7). Size markers are at left. The time of exposure at −80°C with an intensifying screen for autoradiograms *A–D* was 16–48 hr, and for *E*, 1 hr. Sk. mus., skeletal muscle.

Comparison of HPTPσ, HPTPδ, and LAR PTPase Activities. To establish that HPTPσ has PTPase activity and to compare its activity with that of HPTPδ and LAR, the intracellular regions of these three proteins were expressed as

Table 1. PTPase activities of HPTPσ, HPTPδ, and LAR

Fusion protein*	PTPase activity, units/mg of fusion protein		
	MBP	Raytide	MBP/Raytide
GST-HPTPσ (1342–1919)	140,000	9,400	14.9
GST-HPTPδ (1279–1892)	65,600	4,700	14.0
GST-LAR (1275–1881)	234,000	9,600	24.4
GST-CD45 (584–1281)	441,000	1,110,000	0.4
GST	<30	<20	

PTPase assays were done with purified GST fusion proteins and [^{32}P]phosphotyrosine-labeled MBP or Raytide peptide substrates at 37°C for 30 min as described (24).

*Numbers in parentheses indicated the amino acid residues of the PTPases fused to GST.

Table 2. Assay of interaction of LIP.1 with LAR, HPTPδ, and HPTPσ

Bait	Interactor	β-Gal units
LAR-D1D2 (1275–1881)	LIP.1 (794–1185)	176
LAR-D2 (1530–1881)	LIP.1 (794–1185)	143
HPTPδ-D2 (1624–1892)	LIP.1 (794–1185)	554
LIP.1 (794–1185)	LAR (964–1881)	1835
LIP.1 (794–1185)	HPTPσ-D2 (1586–1919)	184
LAR-D1 (1275–1715)	LIP.1 (794–1185)	<10
CD45 (584–1281)	LIP.1 (794–1185)	<10

The interaction trap assay was performed as described (25). Numbers in parentheses are the amino acid residues of the PTPases and LIP.1 fused to the LexA DNA-binding domain (the baits) or to the B42 transcription activation domain (the interactors). The interactors LAR (964–1881) and HPTPσ-D2 (1586–1919) were isolated by screening a cDNA library with LIP.1 (794–1185) as bait. Measurements of β-galactosidase (β-Gal) levels in liquid cultures were done in duplicate from two independent isolates, and the average values of β-Gal units are shown.

GST fusion proteins and purified by glutathione-Sepharose chromatography. HPTPσ, as well as HPTPδ, LAR, and leukocyte CD45 PTPase, dephosphorylated the [^{32}P]phosphotyrosine-containing MBP and Raytide peptide substrates (Table 1). The approximate specific activity and *in vitro* substrate preference (i.e., the MBP/Raytide activity ratios) were similar for HPTPσ, HPTPδ, and LAR (but different for CD45), suggesting that these three enzymes may act upon similar substrates.

Interaction of HPTPσ, HPTPδ, and LAR with the Coiled-Coil Protein LIP.1. We recently characterized a coiled-coil phosphoserine protein, LIP.1, that interacts with the membrane-distal LAR D2 PTPase domain and colocalizes with LAR to focal adhesions (21). To determine whether HPTPδ and HPTPσ might also interact with LIP.1, the interaction between LIP.1 and the intracellular regions of LAR, HPTPσ, and HPTPδ was tested. LAR, HPTPδ, and HPTPσ, but not CD45, interacted with LIP.1 in the interaction trap assay (25) (Table 2). Further, the 160-kDa LIP.1 was specifically precipitated from cell lysates by the LAR-, HPTPδ-, and HPTPσ-GST fusion proteins, but not by the CD45-GST fusion protein (Fig. 5). These results suggest that HPTPσ and HPTPδ also interact with LIP.1 *in vivo*. LIP.1 does not appear to be a PTPase substrate but may function to link LAR, and possibly HPTPσ and PTPδ, to other proteins, including putative substrates and/or is important for recruiting these PTPases to focal adhesion. Further, as LAR and LIP.1 asymmetrically decorate focal adhesions and are excluded from the distal ends, thus localizing to regions of focal adhesions presumably undergoing disassembly (21), it is suggested that HPTPσ and HPTPδ may also play a similar role in regulating turnover of focal adhesions.

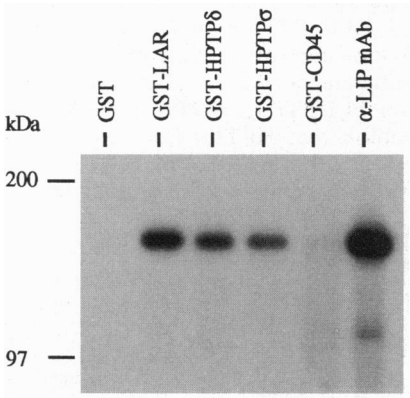

FIG. 5. Binding of LIP.1 to LAR-, HPTPδ-, and HPTPσ-GST fusion proteins. Shown is SDS/PAGE analysis of proteins precipitated by LAR-, HPTPδ-, HPTPσ-, and CD45-GST fusion proteins, control GST protein, or the anti-LIP.1.77 monoclonal antibody (α-LIP mAb) from lysates of ^{35}S-labeled COS-7 cells transfected with the pMT.2.LIP.1b expression vector, which encodes the 160-kDa LIP.1. The GST-PTPase fusion proteins did not precipitate any detectable proteins from ^{35}S-labeled, vector-only-transfected COS-7 cells (data not shown). Molecular mass markers are at left.

We thank Drs. Paul Anderson, Nancy Kedersha, Neil Krueger, and Haruo Saito for critical review of the manuscript and helpful suggestions. We thank Dr. Stuart F. Schlossman for encouragement and support. This work was supported by Grant CA55547 from the National Institutes of Health to M.S., a postdoctoral fellowship award from the Fundación Ramón Areces (Spain) to R.P., a Fulbright fellowship award from the Ministerio de Educación y Ciencia (Spain) to C.S.-P., and a Pew Scholar in the Biomedical Sciences award to M.S.

1. Fischer, E. H., Charbonneau, H. & Tonks, N. K. (1991) *Science* **253**, 401–406.
2. Schlessinger, J. & Ullrich, A. (1992) *Neuron* **9**, 383–391.
3. Hunter, T. (1995) *Cell* **80**, 225–236.
4. Clark, E. A. & Brugge, J. S. (1995) *Science* **268**, 233–239.
5. Saito, H. & Streuli, M. (1991) *Cell Growth Differ.* **2**, 59–65.
6. Trowbridge, I. S. & Thomas, M. L. (1994) *Annu. Rev. Immunol.* **12**, 85–116.
7. Streuli, M., Krueger, N. X., Hall, L. R., Schlossman, S. F. & Saito, H. (1988) *J. Exp. Med.* **168**, 1523–1530.
8. Yu Q., Lenardo, T. & Weinberg, R. A. (1992) *Oncogene* **7**, 1051–1057.
9. Mizuno, K., Hasegawa, K., Katagiri, T., Ogimoto, M., Ichikawa, T. & Yakura, H. (1993) *Mol. Cell. Biol.* **13**, 5513–5523.
10. Pulido, R., Krueger, N. X., Serra-Pages, C., Saito, H. & Streuli, M. (1995) *J. Biol. Chem.* **270**, 6722–6728.
11. Yan, H., Grossman, A., Wang, H., D'Eustachio, P., Mossie, K., Musacchio, J. M., Silvennoinen, O. & Schlessinger, J. (1993) *J. Biol. Chem.* **268**, 24880–24886.
12. Wagner, J., Boerboom, D. & Tremblay, M. L. (1994) *Eur. J. Biochem.*, **226**, 773–782.
13. Gebbink, M. F. B. G., van Etten, I., Hateboer, G., Suijkerbuijk, R., Beijersbergen, R. L., van Kessel, A. G. & Moolenaar, W. H. (1991) *FEBS Lett.* **290**, 123–130.
14. Jiang, Y.-P., Wang, H., D'Eustachio, P., Musacchio, J. M., Schlessinger, J. & Sap, J. (1993) *Mol. Cell. Biol.* **13**, 2942–2951.
15. Krueger, N. X., Streuli, M. & Saito, H. (1990) *EMBO J.* **9**, 3241–3252.
16. Edelman, G. M. & Crossin, K. L. (1991) *Annu. Rev. Biochem.* **60**, 155–190.
17. Stitt, T. N., Conn, G., Gore, M., Lai, C., Bruno, J., *et al.* (1995) *Cell* **80**, 661–670.
18. Brady-Kalnay, S. M., Flint, A. J. & Tonks, N. K. (1993) *J. Cell Biol.* **122**, 961–972.
19. Sap, J., Jiang, Y.-P., Friedlander, D., Grumet, M. & Schlessinger, J. (1994) *Mol. Cell. Biol.* **14**, 1–9.
20. Gebbink, M. F. B. G., Zondag, G. C. M., Wubbolts, R. W., Beijersbergen, R. L., van Etten, I. & Moolenaar, W. H. (1993) *J. Biol. Chem.* **268**, 16101–16104.
21. Serra-Pages, C., Kedersha, N. K., Fazikas, L., Medley, Q., Debant, A. & Streuli, M. (1995) *EMBO J.* **14**, 2827–2838.
22. Chomczynski, P. & Sacchi, N. (1987) *Anal. Biochem.* **162**, 156–159.
23. Streuli, M., Hall, L. R., Saga, Y., Schlossman, S. F. & Saito, H. (1987) *J. Exp. Med.* **166**, 1548–1566.
24. Streuli, M., Krueger, N. X., Thai, T., Tang, M. & Saito, H. (1990) *EMBO J.* **9**, 2399–2407.
25. Gyuris, J., Golemis, E., Chertkov, H. & Brent, R. (1993) *Cell* **75**, 791–803.
26. Pan, M.-G., Rim, C., Lu, K. P., Florio, T. & Stork, P. J. S. (1993) *J. Biol. Chem.* **268**, 19284–19291.
27. Walton, K. M., Martell, K. J., Kwak, S. P., Dixon, J. E. & Largent, B. L. (1993) *Neuron* **11**, 387–400.
28. Zhang, W.-R., Hashimoto, N., Ahmad, F. Ding, W. & Goldstein, B. J. (1994) *Biochem. J.* **302**, 39–47.
29. Ogata, M., Sawada, M., Kosugi, A. & Hamaoka, T. (1994) *J. Immunol.* **153**, 4478–4487.
30. O'Grady, P., Krueger, N. X., Streuli, M. & Saito, H. (1994) *J. Biol. Chem.* **269**, 25193–25199.
31. von Heijne, G. (1986) *Nucleic Acids Res.* **14**, 4683–4690.
32. Streuli, M., Krueger, N. X., Ariniello, P. D., Tang, M., Munro, J. M., Blattler, W. A., Adler, D. A., Disteche, C. M. & Saito, H. (1992) *EMBO J.* **11**, 897–907.
33. Zhang, J. S. & Longo, F. M. (1995) *J. Cell Biol.* **128**, 415–431.
34. Williams, A. F. & Barclay, A. N. (1988) *Annu. Rev. Immunol.* **6**, 381–405.
35. Doherty, P., Moolenaar, C. E. C. K., Ashton, S. V., Michalides, R. J. A. M. & Walsh, F. S. (1992) *Nature (London)* **356**, 791–793.
36. Grumet, M., Mauro, V., Burgoon, M. P., Edelman, G. M. & Cunningham, B. A. (1991) *J. Cell Biol.* **113**, 1399–1412.
37. Volkmer, H., Hassel, B., Wolff, J. M., Frank, R. & Rathjen, F. G. (1992) *J. Cell Biol.* **118**, 149–161.